KA–TP–11–1997
DFPD/97/28
hep-ph/9707437
July 1997

One–loop MSSM Contribution to the Weak Magnetic Dipole Moments of Heavy Fermions

W. Hollik[a], J.I. Illana[a], S. Rigolin[a,b], D. Stöckinger[a] *

[a] Institut für Theoretische Physik, Universität Karlsruhe,
D–76128 Karlsruhe, FR Germany

[b] Dipartimento di Fisica, Università di Padova and INFN,
I-35131 Padua, Italy

Abstract

The MSSM predictions at the one-loop level for the weak-magnetic dipole moments of the τ lepton and the b quark are analysed. The entire supersymmetric parameter space is scanned with the usual GUT constraint and common squark and slepton mass parameters. The real part of a_τ^W is dominated by the chargino contribution, being the same order as the SM one or even larger in the high $\tan\beta$ region whereas the imaginary part, due to Higgs boson diagrams, is negligible compared to the SM value. The real part of a_b^W is controlled mainly by charginos and also by gluinos, when the mixing in the bottom squark sector is large, to yield, for high $\tan\beta$, a contribution one order of magnitude larger than the pure electroweak SM value but a factor five smaller than the standard QCD contribution. The imaginary part of a_b^W is the same order as in the SM.

*E-mail addresses: {hollik,jillana,ds}@itpaxp3.physik.uni-karlsruhe.de, rigolin@pd.infn.it

The investigation of the electric and magnetic dipole moments provides very accurate tests of the quantum structure of the Standard Model (SM) (see [1] and references therein) and of possible extensions (see [2, 3] and references therein). The fermion-Z boson vertex, in higher order, involves coupling terms which in their Lorentz structure are analogous to the magnetic and electric dipole terms of the fermion-photon vertex with valuable informations on the CP-conserving and CP-violating sectors of the SM. In addition, the magnetic weak dipole terms exhibit non-decoupling properties [4] when the top quark is involved in the quantum contributions. Together with the chirality-flipping character of the dipole form factors one thus might expect also some insight into the mechanism of mass generation. Extensions of the minimal model by new renormalizable interactions influence the dipole form factors by non-standard loop contributions. In this article we consider the Minimal Supersymmetric Standard Model (MSSM) as a particularly interesting extension of the SM and investigate the impact of the MSSM one-loop contributions to the weak-magnetic dipole moments of heavy fermions.

The most general Lorentz structure of the vertex function that couples a Z boson and two on-shell fermions (with outgoing momenta q and $\bar{q}$) can be written as

$$\begin{aligned} \Gamma_\mu^{Zff} &= ie\Big\{\gamma_\mu\left[\left(F_{\rm V}-\frac{v_f}{2s_Wc_W}\right)-\left(F_{\rm A}-\frac{a_f}{2s_Wc_W}\right)\gamma_5\right] \\ &\quad +(q-\bar{q})_\mu[F_{\rm M}+F_{\rm E}\gamma_5]-(q+\bar{q})_\mu[F_{\rm S}+F_{\rm P}\gamma_5]\Big\}\,, \end{aligned} \tag{1}$$

where $v_f \equiv (I_3^f - 2s_W^2Q_f)$, $a_f \equiv I_3^f$ (the weak isospin of the fermion) and $s_W^2 \equiv 1-c_W^2 \equiv \sin^2\theta_W$. The form factors $F_i(s)$ are defined splitting off the tree level SM terms, and depend only on $s \equiv p^2 = (q+\bar{q})^2$. Conservation of the vector current (U(1) gauge invariance) constrains the scalar form factor $F_{\rm S}$ to be zero at $s = M_Z^2$. The axial form factor $F_{\rm P}(M_Z^2)$ must also vanish for massless fermions. The vector and axial-vector form factor, $F_{\rm V}$ and $F_{\rm A}$, are the only ones that have to be renormalized while the others are finite. The form factors $F_{\rm M}$ and $F_{\rm E}$ are related to the weak dipole moments of the fermion f with mass m_f as follows [5]:

$$\begin{aligned} \text{AWMDM} \equiv a_f^W &= -2m_f\; F_{\rm M}(M_Z^2)\,, \\ \text{WEDM} \equiv d_f^W &= ie\; F_{\rm E}(M_Z^2)\,. \end{aligned}$$

The anomalous weak-magnetic dipole moment (AWMDM) is the analogue of the anomalous magnetic dipole moment (AMDM) $a_f^\gamma = (g_f-2)/2$. The $F_{\rm M}$ ($F_{\rm E}$) form factors are the coefficients of the *chirality-flipping* term of the CP-conserving (CP-violating) effective Lagrangian describing Z-fermion couplings. Therefore, they are expected to get contributions proportional to some positive power of the mass of the fermions involved. This allows the construction of observables which can be probed experimentally most suitably by heavy fermions. Hence, for on-shell Z bosons, where the dipole form factors are gauge independent, the b quark and τ lepton are the most promising candidates.

The contribution to the AWMDM, for the τ lepton and for heavy quarks, at the one-loop level has recently been calculated by Bernabéu et al. in the SM [4, 6] and in two Higgs doublet models [7] . In this letter, we extend these calculations to the MSSM and investigate the maximum size of the non-standard contributions. We classify all the triangle diagrams in six topologies (classes) or generic diagrams (Fig. 1) as in Ref [8]. Working in the 't Hooft-Feynman gauge all the would-be-Goldstone bosons are included. The global result, adding all the diagrams, is gauge independent. Every class of diagrams is calculated analytically for general couplings and expressed in terms of standard one-loop integrals $\bar{C}$ [8] and vertex coefficients λ as follows:

- Class Ia: $\bar{C} = \bar{C}(-\bar{q}, q, \tilde{m}, \tilde{m}, M)$,

$$F_{\rm M}^{\rm Ia}(s) = \frac{\alpha}{4\pi}\{4m_f\lambda_V^+[-2C_2^+ + 3C_1^+ - C_0] + 4\tilde{m}\lambda'_V[-2C_1^+ + C_0]\} \;, \qquad (2)$$

  with $\lambda_V^{\pm} = V(V'^2 + A'^2) \pm 2AV'A'$, $\lambda'_V = V(V'^2 - A'^2)$.

- Class Ib: $\bar{C} = \bar{C}(-\bar{q}, q, m_f, m_f, 0)$

$$F_{\rm M}^{\rm Ib}(s) = C_{\rm F}\frac{\alpha_s}{4\pi}\{V[4m_f(-2C_2^+ + 3C_1^+ - C_0) + 4\tilde{m}(-2C_1^+ + C_0)]\} \;. \qquad (3)$$

  The colour factor $C_{\rm F} = \frac{4}{3}$.

- Class II: $\bar{C} = \bar{C}(-\bar{q}, q, M, M, \tilde{m})$,

$$F_{\rm M}^{\rm II}(s) = \frac{\alpha}{4\pi}\{2m_f\lambda_V[4C_2^+ + C_1^+] - 6\tilde{m}\lambda'_V C_1^+\} \;, \qquad (4)$$

  with $\lambda_V = G(V^2 + A^2)$, $\lambda'_V = G(V^2 - A^2)$.

- Class III: $\bar{C} = \bar{C}(-\bar{q}, q, \tilde{m}_1, \tilde{m}_2, M)$,

$$F_{\rm M}^{\rm III}(s) = \frac{\alpha}{4\pi}\{-2m_f\lambda_V^+[2C_2^+ - C_1^+] + (\tilde{m}_1 + \tilde{m}_2)\lambda'_V C_1^+ + (\tilde{m}_1 + \tilde{m}_2)\lambda''_A C_1^- + (\tilde{m}_1 - \tilde{m}_2)\lambda''_A C_1^+ + (\tilde{m}_1 - \tilde{m}_2)\lambda'_V C_1^-\} \;, \qquad (5)$$

  with $\lambda_V^{\pm} = V(SS' - PP') \pm A(SP' - PS')$, $\lambda'_V = V(SS' + PP')$, $\lambda''_A = A(SP' + PS')$.

- Class IV: $\bar{C} = \bar{C}(-\bar{q}, q, M_1, M_2, \tilde{m})$,

$$F_{\rm M}^{\rm IV}(s) = \frac{\alpha}{4\pi}\{2m_f\lambda_V[2C_2^+ - C_1^+] + \tilde{m}\lambda'_V[2C_1^+ - C_0]\} \;, \qquad (6)$$

  with $\lambda_V = G(SS' - PP')$, $\lambda'_V = G(SS' + PP')$.

- Class V: $\bar{C} = \bar{C}(-\bar{q}, q, M_1, M_2, \tilde{m})$,

$$F_{\rm M}^{\rm V}(s) = \frac{\alpha}{4\pi}\{\lambda_V[C_1^+ + C_1^-]\} , \quad (7)$$

with $\lambda_V = G(SV + PA)$.

- Class VI: $\bar{C} = \bar{C}(-\bar{q}, q, M_1, M_2, \tilde{m})$,

$$F_{\rm M}^{\rm VI}(s) = \frac{\alpha}{4\pi}\{\lambda_V[C_1^+ - C_1^-]\} , \quad (8)$$

with $\lambda_V = G(SV - PA)$.

We use the conventions of Refs. [9] for the couplings, masses and vertex coefficients.[1] We employ the compact notation $a_f^W[ijk]$ for the contribution to the AWMDM of particles i, j, k running in the loop as labelled in Fig. C.1 of Ref. [8]. Notice that all the masses appearing explicitly as factors of the $\bar{C}$ integrals in the expressions are fermion masses, consistently with the chirality flipping character of the dipole moments.

The WMDM of the τ lepton

In the SM there are 14 diagrams at one-loop, in the 't Hooft-Feynman gauge, contributing to the τ-Z boson coupling. We are in agreement[2] with Ref. [6] with the total value for $M_{H^0} = 2M_Z$, $m_\tau = 1.777$ GeV, $M_Z = 91.19$ GeV, $s_W^2 = 0.232$ and $\alpha = 1/128$:

$$a_\tau^W[\text{SM}] = (2.10 + 0.61\ i) \times 10^{-6} .$$

The diagrams with Higgs bosons have only a small impact, changing the final result [6] by less than 1% for $1 < M_{H^0}/M_Z < 3$.

The MSSM contributions introduce new parameters, the values of which are not known but are constrained by present experiments. To reduce the number of free parameters, we assume the usual GUT constraint for the soft-breaking mass terms in the gaugino sector and a common squark mass parameter as well as a common slepton mass parameter. For given $\tan\beta$, we are left with the following free parameters: the gaugino mass parameter for the SU(2) sector M, the Higgs-higgsino mass parameter μ, the common slepton soft-breaking mass parameter $m_{\tilde{l}}$, the common squark soft-breaking mass parameter $m_{\tilde{q}}$, the trilinear soft-breaking term A_τ and the mass of the pseudoscalar Higgs boson M_A. We consider two typical scenarios: low and high $\tan\beta$, respectively $\tan\beta = 1.6$ and 50. The genuine MSSM diagrams to be included are: diagrams with MSSM Higgs bosons; diagrams with charginos and scalar neutrinos; and diagrams with neutralinos and $\tilde{\tau}$ sleptons.

[1] This leads to the different signs of the tree level part of Eq. (1) when compared to Eq. (3.14) of Ref. [8].

[2] The global sign is due to our different conventions.

MSSM Higgs contribution to a_τ^W

The diagrams for $Z\tau\tau$ involving Higgs bosons are:

class III: $[\tau\tau h]$, $[\tau\tau H]$, $[\tau\tau A]$, $[\tau\tau G^0]$, $[\nu\nu H^-]$, $[\nu\nu G^-]$,

class IV: $[Ah\tau]$, $[G^0h\tau]$, $[AH\tau]$, $[G^0H\tau]$, $[hA\tau]$, $[hG^0\tau]$, $[HA\tau]$, $[HG^0\tau]$, $[H^-H^-\nu]$, $[H^-G^-\nu]$, $[G^-H^-\nu]$, $[G^-G^-\nu]$,

class V: $[Zh\nu]$, $[ZH\nu]$, $[WG^-\nu]$,

class VI: $[hZ\nu]$, $[HZ\nu]$, $[G^-W\nu]$,

where G^0, $G^\pm$ are the would-be-Goldstone bosons and h, H, A and $H^\pm$ are the physical MSSM Higgs bosons. Actually, not all of them give a contribution to the AWMDM, in particular, the diagrams of class IV with neutral Higgs bosons vanish as in the case of the SM. The masses of the Higgs bosons are fixed by the mass of the pseudoscalar, M_A, $\tan\beta$ and the common squark mass parameter $m_{\tilde{q}}$, which are the only free parameters involved in this calculation. A value $m_{\tilde{q}} = 250$ GeV will be assumed in the following. Low values of M_A yield the largest contribution and for $M_A \gtrsim 300$ GeV the contributions become M_A-independent. The class III diagrams provide the only contribution to $\mathrm{Im}(a_\tau^W)$, assuming the present lower bound for the masses of the Higgs bosons [11]. Due to the fact that the ratio of vector couplings v_τ/v_ν is small, the diagrams with charged Higgs bosons give the main contribution, which is of the order $\alpha/4\pi(m_\tau/M_Z)^4\ \tan^2\beta \sim 10^{-10}$ (10^{-7}) for the low (high) $\tan\beta$ scenario. For example, one gets

$$\mathrm{Im}(a_\tau^W[\mathrm{Higgs}]) = -0.0001\ (0.06) \times 10^{-6} \text{ for } M_A = 100 \text{ GeV and low (high)} \tan\beta\ .$$

For $\mathrm{Re}(a_\tau^W)$, the diagrams of classes III and IV are proportional to $(m_\tau/M_Z)^4\tan^2\beta$ and the diagrams of classes V and VI are proportional to $(m_\tau/M_Z)^2$. Actually,

$$\mathrm{Re}(a_\tau^W[\mathrm{Higgs}]) = \left\{ \begin{array}{l} -0.3\ (-0.4) \times 10^{-6} \text{ for } M_A = 100 \text{ GeV} \\ -0.3\ (-0.3) \times 10^{-6} \text{ for } M_A \gtrsim 300 \text{ GeV} \end{array} \right. \text{ for low (high) } \tan\beta\ .$$

Chargino and scalar neutrino contribution to a_τ^W

There are two diagrams involving charginos and scalar neutrinos:

class III: $[\tilde{\chi}_i^-\tilde{\chi}_j^-\tilde{\nu}]$,

class IV: $[\tilde{\nu}\tilde{\nu}\tilde{\chi}_k^-]$.

Charginos [12] and scalar neutrinos [13] do not occur in Z decays and hence their contribution to the AWMDM is real, in the region of their masses not ruled out by the experiments. The free parameters involved here are $\tan\beta$, M, μ and $m_{\tilde{l}}$. The contribution becomes smaller increasing $m_{\tilde{l}}$ (consistently with decoupling [10]). In the large M and $|\mu|$ region the charginos also decouple. The contribution is enhanced by increasing $\tan\beta$. In the low $\tan\beta$ scenario the contribution is of order 10^{-7}. The value for $m_{\tilde{l}} = 250$ GeV, $M = 200$ GeV and $|\mu| = 200$ GeV is

$$\mathrm{Re}(a_\tau^W[\text{charginos}]) = \begin{cases} -0.2 \times 10^{-6} \ (\mu < 0) \\ +0.2 \times 10^{-6} \ (\mu > 0) \end{cases} \quad \text{for low } \tan\beta \ .$$

In the high $\tan\beta$ scenario the contribution is of order 10^{-5}. We find:

$$\mathrm{Re}(a_\tau^W[\text{charginos}]) = \begin{cases} -7.0 \times 10^{-6} \ (\mu < 0) \\ +7.0 \times 10^{-6} \ (\mu > 0) \end{cases} \quad \text{for high } \tan\beta$$

and the same values for M and $|\mu|$ as above. This enhancement for higher $\tan\beta$ is expected in analogy to the AMDM of the muon. The contours in the $M - \mu$ plane are similar to the ones for the b quark (Fig. 2) suppressed by factors between m_τ/m_b and $(m_\tau/m_b)^2$ [see Eqs. (5) and (6)].

Neutralino and $\tilde{\tau}$ slepton contribution to a_τ^W

There are two diagrams involving neutralinos and $\tilde{\tau}$ sleptons:

class III: $[\tilde{\chi}_i^0 \tilde{\chi}_j^0 \tilde{\tau}_k]$,

class IV: $[\tilde{\tau}_i \tilde{\tau}_j \tilde{\chi}_k^0]$.

The $\tilde{\tau}$ slepton masses are bounded by present experiments [14] to be heavier than half the mass of the Z, but the neutralinos are less stringently bounded and could be much lighter [12], allowing for the possibility of a contribution to the imaginary part of the AWMDM through diagrams of class III. Now, we have $\tan\beta$, M, μ, $m_{\tilde{l}}$, as well as the trilinear soft-breaking mass term for the $\tilde{\tau}$ sleptons, A_τ, as free parameters. We choose different values for A_τ in the range $\pm\mu\tan\beta$ to estimate the sensitivity of the AWMDM to this soft-breaking term and find no sizeable deviation. However, for some values of A_τ and μ the mass of the $\tilde{\tau}$ sleptons can become unphysical. For simplicity, we take the value of A_τ that makes $m_{LR}^\tau = A_\tau - \mu\tan\beta = 0$. Just below the neutralino threshold the imaginary part is

$$|\mathrm{Im}(a_\tau^W[\text{neutralinos}])| \sim 10^{-9} \ (10^{-7}) \text{ for low (high) } \tan\beta$$

and it is negligible far below threshold. Concerning the real part, also the value is maximum near the neutralino pair threshold. Like in the chargino-scalar neutrino contributions, the result is expected to be enhanced by $\tan\beta$. We find

$$\mathrm{Re}(a_\tau^W[\text{neutralinos}]) = -0.02(-0.4) \times 10^{-6} \text{ for low (high) } \tan\beta$$

and $M = \mu = 200$ GeV.

The WMDM of the b quark

In the electroweak SM there are 14 diagrams, in the 't Hooft-Feynman gauge, contributing to the b-Z boson coupling at the one-loop level, plus one more (gluon exchange) if QCD is also included. Our calculation reproduces the result of Ref. [4]. Taking as input $m_b = 4.5$ GeV, $m_t = 175$ GeV, $M_Z = 91.19$ GeV, $s_W^2 = 0.232$, $\alpha = 1/128$ and $\alpha_s = 0.118$, the pure electroweak contribution is $a_b^W(\mathrm{EW}) = [(1.1;\ 2.0;\ 2.4) - 0.2\ i] \times 10^{-6}$, for $M_{H^0} = M_Z,\ 2M_Z,\ 3M_Z$, but the whole value is dominated by the QCD contribution to give

$$a_b^W[\mathrm{EW}+\mathrm{QCD}] = (-2.98 + 1.56\ i) \times 10^{-4}\ .$$

Only the third generation of quarks is considered and the element V_{tb} of the CKM matrix is set to 1.

In the MSSM one has to include the following genuine supersymmetric contributions: diagrams with MSSM Higgs bosons; diagrams with charginos and $\tilde{t}$ squarks; diagrams with neutralinos and $\tilde{b}$ squarks; and diagrams with gluinos and $\tilde{b}$ squarks. In this case, we are left with the following free parameters: M, μ, $m_{\tilde{q}}$, M_A, the trilinear soft-breaking terms A_b and A_t and a mass for the gluinos $m_{\tilde{g}}$.

MSSM Higgs contribution to a_b^W

The diagrams for Zbb involving Higgs bosons are

class III: $[bbh]$, $[bbH]$, $[bbA]$, $[bbG^0]$, $[ttH^-]$, $[ttG^-]$,

class IV: $[Ahb]$, $[G^0hb]$, $[AHb]$, $[G^0Hb]$, $[hAb]$, $[hG^0b]$, $[HAb]$, $[HG^0b]$, $[H^-H^-t]$, $[H^-G^-t]$, $[G^-H^-t]$, $[G^-G^-t]$,

class V: $[Zht]$, $[ZHt]$, $[WG^-t]$,

class VI: $[hZt]$, $[HZt]$, $[G^-Wt]$.

As before, the diagrams of class IV with neutral Higgs bosons do not contribute. The diagrams of class III with neutral Higgs bosons yield $\mathrm{Im}(a_b^W) \sim \alpha/4\pi(m_b/M_Z)^4 \tan^2\beta \sim 10^{-8}$ (10^{-6}) for low (high) $\tan\beta$. Taking $m_{\tilde{q}} = 250$ GeV we get

$$\mathrm{Im}(a_b^W[\mathrm{Higgs}]) = \begin{cases} 0.02\ (3.7) \times 10^{-6} \text{ for } M_A = 100 \text{ GeV} \\ 0.01\ (0.08) \times 10^{-6} \text{ for } M_A = 300 \text{ GeV} \end{cases} \text{and low (high) } \tan\beta\ .$$

Concerning $\mathrm{Re}(a_b^W)$, there are contributions proportional to $\left(\frac{m_b}{M_Z}\right)^2$, $\left(\frac{m_b m_t}{M_Z^2}\right)^2$ and $\left(\frac{m_b}{M_Z}\right)^4 \tan^2\beta$. The sum is thus not very sensitive to $\tan\beta$,

$$\mathrm{Re}(a_b^W[\mathrm{Higgs}]) = \begin{cases} -3.8\ (+0.8) \times 10^{-6} \text{ for } M_A = 100 \text{ GeV} \\ -1.8\ (-0.9) \times 10^{-6} \text{ for } M_A = 300 \text{ GeV} \end{cases} \text{and low (high) } \tan\beta\ .$$

Chargino and $\tilde{t}$ squark contribution to a_b^W

There are two diagrams involving charginos and $\tilde{t}$ squarks:

class III: $[\tilde{\chi}_i^- \tilde{\chi}_j^- \tilde{t}_k]$,

class IV: $[\tilde{t}_i \tilde{t}_j \tilde{\chi}_k^-]$.

As in the τ case, assuming the present bounds on chargino and squark masses [12, 15], $\mathrm{Im}(a_b^W[\mathrm{charginos}])$=0. The free parameters involved are $\tan\beta$, M, μ, $m_{\tilde{q}}$ and A_t. Varying the value for A_t in the range $\pm\mu\cot\beta$ shows that there is only a small effect in the AWMDM. We thus choose A_t in a way that the off-diagonal entry of the $\tilde{t}$ squarks mixing mass matrix $m_{LR}^t = A_t - \mu\cot\beta = 0$. Increasing $m_{\tilde{q}}$ the contribution becomes smaller. Fig. 2 shows a contour plot in the $M - \mu$ plane for $m_{\tilde{q}} = 250$ GeV. In the large M and $|\mu|$ region, the charginos decouple, as expected from the decoupling theorem [10]. The contour lines for the masses of the lightest chargino and lightest neutralino in the $M - \mu$ plane are also depicted. The contributions are enhanced by increasing $\tan\beta$. In the low $\tan\beta$ scenario the contribution is of order 10^{-6} (Fig. 2a). For $M = |\mu|$=200 GeV we get

$$\mathrm{Re}(a_b^W[\mathrm{charginos}]) = \begin{cases} -1.1 \times 10^{-6}\ (\mu < 0) \\ 1.0 \times 10^{-6}\ (\mu > 0) \end{cases} \text{for low } \tan\beta\ .$$

In the high $\tan\beta$ scenario (Fig. 2b) the contribution is enhanced to become of order 10^{-5}. For the same values of M and μ as above,

$$\mathrm{Re}(a_b^W[\mathrm{charginos}]) \simeq \begin{cases} -32.2 \times 10^{-6}\ (\mu < 0) \\ +33.6 \times 10^{-6}\ (\mu > 0) \end{cases} \text{for high } \tan\beta\ .$$

Neutralino and $\tilde{b}$ squark contribution to a_b^W

There are two diagrams involving neutralinos and $\tilde{b}$ squarks:

class III: $[\tilde{\chi}_i^0 \tilde{\chi}_j^0 \tilde{b}_k]$,

class IV: $[\tilde{b}_i \tilde{b}_j \tilde{\chi}_k^0]$.

Now, we have $\tan\beta$, M, μ, $m_{\tilde{q}}$, as well as the trilinear soft-breaking mass term for the $\tilde{b}$ squarks, A_b, as free parameters. There is no sizeable dependence on A_b. As in the τ case, due to the heavy mass of the $\tilde{b}$ squarks [15], an imaginary part can only arise through diagrams of class III. The region of non vanishing $\mathrm{Im}(a_b^W)$ is below the neutralino threshold and the value is

$$|\mathrm{Im}(a_b^W[\text{neutralinos}])| \sim 0.1(1) \times 10^{-6} \text{ for low (high) } \tan\beta \ ,$$

near threshold. Concerning the real part, also the value is maximum near the neutralino pair threshold. The result is proportional to $\tan\beta$ as expected:

$$\mathrm{Re}(a_b^W[\text{neutralinos}]) = -0.2\ (-10.5) \times 10^{-6} \ \text{ for low (high) } \tan\beta$$

and $M = \mu = 200$ GeV.

Gluino contribution to a_b^W

There is one diagram with a gluino and two $\tilde{b}$ squarks running in the loop:

class IV: $[\tilde{b}_i \tilde{b}_j \tilde{g}]$.

The present bounds on $\tilde{b}$ squark masses [15] only allow a real contribution to the AWMDM. The free parameters are $\tan\beta$, $m_{\tilde{q}}$, $m_{\tilde{g}}$, A_b and μ. These last two parameters affect the result only through the off-diagonal term of the $\tilde{b}$ squark mass matrix $m_{LR}^b = A_b - \mu\tan\beta$. There still remains a slight dependence on $\tan\beta$ in the diagonal terms of the $\tilde{b}$ squark mass matrix and so we keep the distinction between low and high $\tan\beta$ scenarios. The mixing in the $\tilde{b}$ sector is determined by m_{LR}^b and intervenes in the contribution due to chirality flipping in the gluino internal line (the contribution proportional to $m_{\tilde{g}}$). Thus, the contribution to the AWMDM is enhanced by the largest values of m_{LR}^b compatible with a physical and experimentally not excluded mass for the lightest $\tilde{b}$ squark. Assuming a typical scale for m_{LR}^b of order $\mu\tan\beta$ leads to values of the order 100 GeV (10 TeV) for the low (high) $\tan\beta$ scenarios.

The low $\tan\beta$ region is displayed in Fig. 3a, for $m_{\tilde{q}} = 250$ GeV. The mixing for the plotted values of m_{LR}^b do not affect significantly the mass of the lightest $\tilde{b}$ squark (always above 200 GeV). For zero gluino mass, only the term proportional to the mass of the b

quark provides a contribution. As we increase the gluino mass, the term proportional to $m_{\tilde{g}}$ dominates, especially for large m^b_{LR}, being again suppressed at high $m_{\tilde{g}}$ due to the gluino decoupling. The typical value is

$$\mathrm{Re}(a_b^W[\mathrm{gluinos}]) = -1.1 \times 10^{-6} \ \text{ for low } \tan\beta$$

and $m_{\tilde{g}} = m^b_{LR} = 200$ GeV. For high $\tan\beta$ (Fig. 3b), the behaviour is analogous but larger values can be obtained. For example, choosing $m_{\tilde{g}} = 200$ GeV and $m^b_{LR} = 7$ TeV, we obtain

$$\mathrm{Re}(a_b^W[\mathrm{gluinos}]) = -18.9 \times 10^{-6} \ \text{ for high } \tan\beta \ .$$

Conclusions

From the previous analysis we conclude that the imaginary part of the AWMDM of the τ lepton is provided only by the diagrams with Higgs bosons, being at most of order 10^{-7} for the high $\tan\beta$ scenario, an order of magnitude below the SM contribution. For the real part, the charginos dominate with a contribution of order 10^{-5} (10^{-6}) in the high (low) $\tan\beta$ scenario at the level of the SM contribution or even larger. The neutralino contribution is of opposite sign, but one order of magnitude smaller. Also the Higgs contribution to the real part is negligible.

The most important MSSM contribution to the a_b^W is provided by charginos and gluinos in the high $\tan\beta$ scenario. For high $\tan\beta$, the neutralino and chargino contributions have opposite sign, but the former is typically a factor five below. On the other hand, the chargino contribution has the sign of μ whereas the gluinos only contribute with negative sign. Therefore the total contribution to the real part is maximal for negative μ and can reach the value of

$$\mathrm{Re}(a_b^W[\mathrm{MSSM}]) \sim -60 \times 10^{-6} \ \text{ for high } \tan\beta \ .$$

These values are one order of magnitude higher than the pure electroweak SM contribution, but still a factor five below the standard QCD contribution. The Higgs boson diagrams are negligible, and they are only important for the imaginary part, contributing the same amount as the neutralinos below threshold, at most

$$|\mathrm{Im}(a_b^W[\mathrm{MSSM}])| \sim 10^{-6} \ \text{ for high } \tan\beta \ .$$

This value is of the same order as the electroweak SM result. In the low $\tan\beta$ scenario, all the MSSM contributions to the real part are of order 10^{-6}; for the imaginary part they are one order of magnitude smaller. They both are comparable in size to the pure electroweak SM contribution.

Acknowledgements

Discussions with F. Feruglio, G.A. González-Sprinberg and A. Masiero are gratefully acknowledged. J.I.I. is supported by the Fundación Ramón Areces and partially by the Spanish CICYT under contract AEN96-1672. S.R. is supported by the Fondazione Ing. A. Gini and by the italian MURST.

References

[1] T. Kinoshita, *Phys. Rev. Lett.* **75** (1995) 4728;
A. Czarnecki, B. Krause, W.J. Marciano, *Phys. Rev.* **D52** (1995) 2619; *Phys. Rev. Lett.* **76** (1996) 3267;
F. Jegerlehner, *Nucl. Phys. Proc. Suppl.* **51C** (1996) 131;
S. Laporta, E. Remiddi *Phys. Lett.* **B379** (1996) 283;
A. Czarnecki, B. Krause, *Phys. Rev. Lett.* **78** (1997) 4339.

[2] Y. Kizukuri, N. Oshimo, *Phys. Rev.* **D45** (1992) 1806; **D46** (1992) 3025;
S. Bertolini, F. Vissani, *Phys. Lett.* **B324** (1994) 164;
T. Inui, Y. Mimura, N. Sakai, T. Sasaki, *Nucl. Phys.* **B449** (1995) 49;
T. Hayashi, Y. Koide, M. Matsuda, M. Tanimoto, *Nucl. Phys. Proc. Suppl.* **39C** (1995) 276;
S.A. Abel, W.N. Cottingham, I.B. Whittingham, *Phys. Lett.* **B370** (1996) 106.

[3] G. Couture, H. König, *Phys. Rev.* **D53** (1996) 555;
U. Chattopadhyay, P. Nath, *Phys. Rev.* **D53** (1996) 1648;
T. Moroi, *Phys. Rev.* **D53** (1996) 6565;
M. Carena, G.F. Giudice, C.E.M. Wagner, *Phys. Lett.* **B390** (1997) 234;
M. Krawczyk, J. Zochowski, *Phys. Rev.* **D55** (1997) 6968.

[4] J. Bernabéu, G.A. González-Sprinberg, J. Vidal, *Phys. Lett.* **B397** (1997) 255.

[5] J. Bernabéu, G.A. González-Sprinberg, J. Vidal, *Phys. Lett.* **B326** (1994) 168;
W. Bernreuther, G.W. Botz, D. Bruss, P. Haberl, O. Nachtmann, *Zeit. für Physik* **C68** (1995) 73;
W. Bernreuther, O. Nachtmann, *Zeit. für Physik* **C73** (1997) 647.

[6] J. Bernabéu, G.A. González-Sprinberg, M.Tung, J. Vidal, *Nucl. Phys.* **B436** (1995) 474.

[7] J. Bernabéu, D. Comelli, L. Lavoura, J. P. Silva, *Phys. Rev.* **D53** (1996) 5222.

[8] W. Beenakker, S.C. van der Marck, W. Hollik, *Nucl. Phys.* **B365** (1991) 24.

[9] H.E. Haber, G.L. Kane, *Phys. Rep.* **117** (1985) 75;
J.F. Gunion, H.E. Haber, *Nucl. Phys.* **B272** (1986) 1 (E: **B402** (1993) 567);
J.F. Gunion, H.E. Haber, G. Kane, S. Dawson, *The Higgs Hunter's Guide*, Addison-Wesley 1990.

[10] T. Appelquist, J. Carrazone, *Phys. Rev.* **D11** (1975) 2856.

[11] OPAL Collaboration, *Zeit. für Physik* **C73** (1997) 189;
ALEPH Collaboration, CERN PPE/97-071.

[12] DELPHI Collaboration, *Phys. Lett.* **B387** (1996) 651; *B396* (1997) 315 ;
OPAL Collaboration, *Phys. Lett.* **B389** (1996) 616; **B393** (1997) 217;
ALEPH Collaboration, CERN PPE/97-041.

[13] ALEPH Collaboration, *Phys. Rep.* **216** (1992) 253;
L3 Collaboration, *Phys. Rep.* **236** (1993) 1.

[14] OPAL Collaboration, *Phys. Lett.* **B396** (1997) 301;
ALEPH Collaboration, CERN PPE/97-056.

[15] DØ Collaboration, *Phys. Rev. Lett.* **75** (1995) 618;
DELPHI Collaboration, *Phys. Lett.* **B387** (1996) 651;
OPAL Collaboration, *Phys. Lett.* **B393** (1997) 217; CERN PPE/97-0461;
CDF Collaboration, FERMILAB-PUB-97/031-E.

Figures

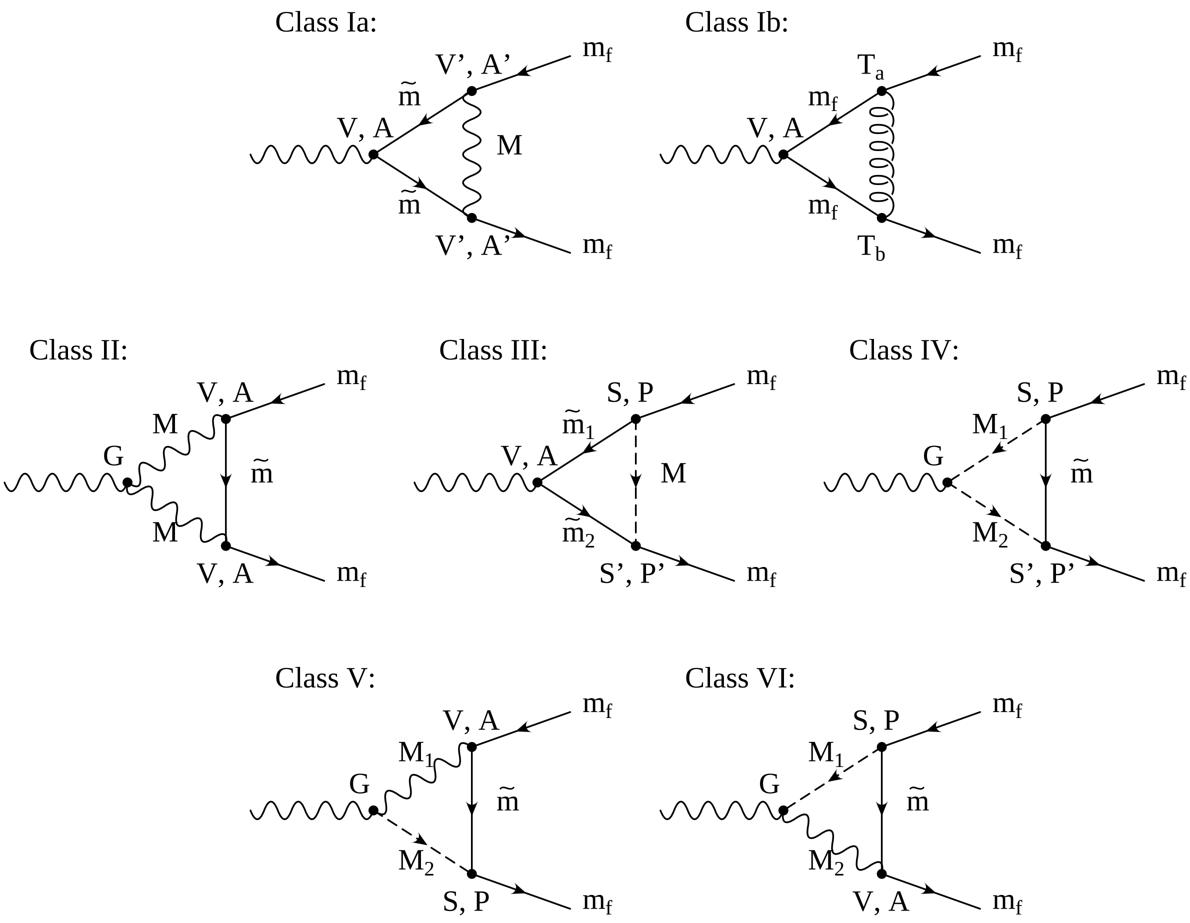

Figure 1: The one-loop Zff diagrams with general couplings.

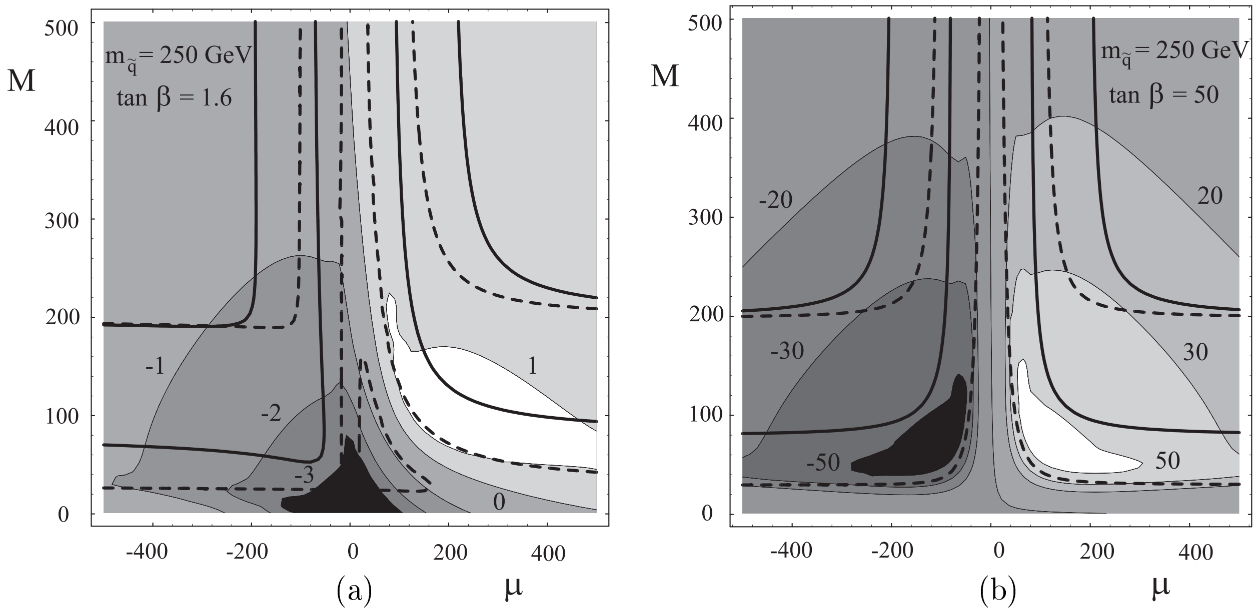

Figure 2: Re(a_b^W[charginos]) for low (a) and high (b) $\tan\beta$ in units of 10^{-6} in the plane $M-\mu$. The contour solid-lines correspond to the light chargino masses $m_{\tilde{\chi}^{\pm}}$=80 and 200 GeV and the contour dashed-lines correspond to the lightest neutralino masses $m_{\tilde{\chi}^0}$=15 and 100 GeV. The common squark mass parameter is fixed to $m_{\tilde{q}} = 250$ GeV and $m^t_{LR} = 0$.

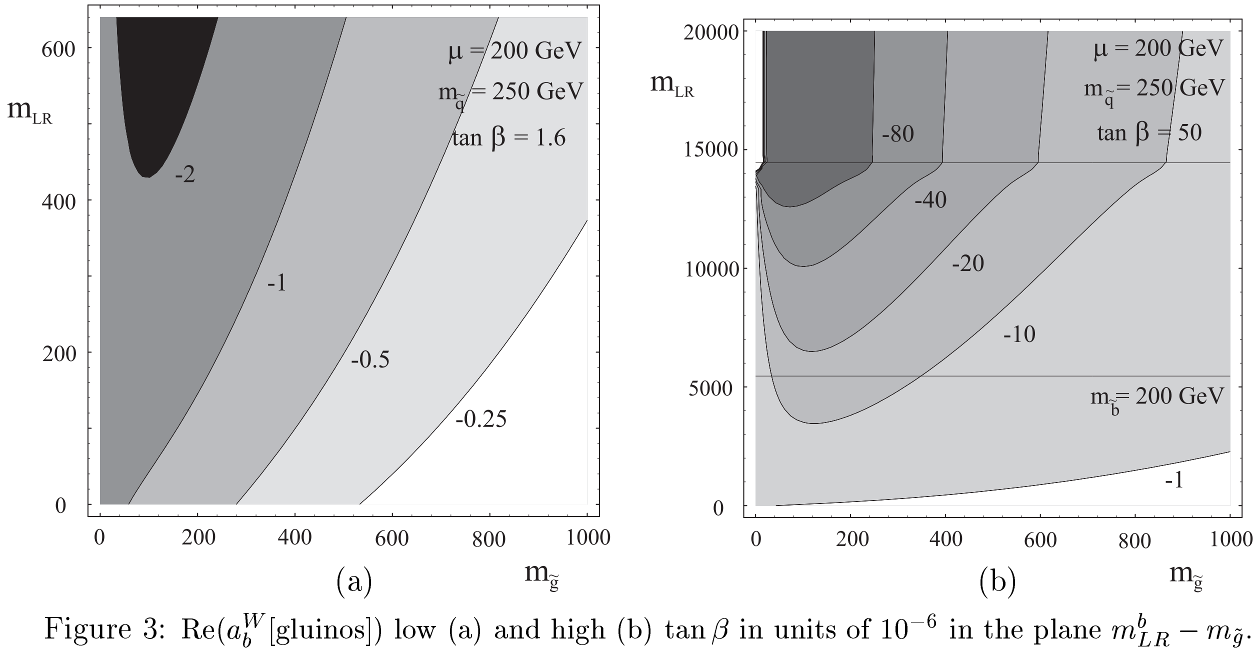

Figure 3: Re(a_b^W[gluinos]) low (a) and high (b) $\tan\beta$ in units of 10^{-6} in the plane $m^b_{LR}-m_{\tilde{g}}$. The common squark mass parameter is fixed to $m_{\tilde{q}} = 250$ GeV. The region above the upper horizontal line is unphysical ($m^2_{\tilde{b}_1} < 0$).